LA-UR- 10-01416

Approved for public release; distribution is unlimited.

Title: Modeling the Mechanical Response of PBX 9501

Author(s): Partha Rangaswamy
Darla G. Thompson
Cheng Liu
Mathew W. Lewis

Intended for: Paper at the
14th International Detonation Symposium
April 11th-16th, 2010, Coeur d'Alene Resort, Idaho
USA

Los Alamos NATIONAL LABORATORY EST.1943

Modeling the mechanical response of PBX 9501

Partha Rangaswamy, Darla G. Thompson, Cheng Liu, Mathew W. Lewis
Los Alamos National Laboratory
Los Alamos, NM 87544

Abstract An engineering overview of the mechanical response of Plastic-Bonded eXplosives (PBXs), specifically PBX 9501, will be provided with emphasis on observed mechanisms associated with different types of mechanical testing. Mechanical tests in the form of uniaxial tension, compression, cyclic loading, creep (compression and tension), and Hopkinson bar show strain rate and temperature dependence. A range of mechanical behavior is observed which includes small strain recoverable response in the form of viscoelasticity; change in stiffness and softening beyond peak strength due to damage in the form microcracks, debonding, void formation and the growth of existing voids; inelastic response in the form of irerecoverable strain as shown in cyclic tests, and viscoelastic creep combined with plastic response as demonstrated in creep and recovery tests. The main focus of this paper is to elucidate the challenges and issues involved in modeling the mechanical behavior of PBXs for simulating thermo-mechanical responses in engineering components. Examples of validation of a constitutive material model based on a few of the observed mechanisms will be demonstrated against three point bending, split Hopkinson pressure bar and Brazilian disk geometry.

Introduction

High explosives (HE) such as Plastic-Bonded eXplosives (PBXs), specifically PBX 9501, are used in a variety of applications. Unexpected explosions of HE can have significant consequences. High explosives provide many structural engineering challenges. In-situ characterization of the stress state and geometry of HE weapon components is one of the most difficult of these challenges.

Predicting the mechanical response of functional energetic materials to stress or strain histories from a first principals approach over a range of environmental conditions is not tractable. The high volume fraction of energetic grains in very dissimilar binders is extremely challenging. Because of the high cost of machining and testing these materials, models have been developed and used with scant data, invoking postulated (but not proven) deformation mechanisms. In general this *ad hoc* model development approach leaves the energetic materials community with dubious predictive capability and no credible means for analyzing the effects of mechanical insults to any given energetic material.

Quasi-static mechanical tests have shown both strain rate and temperature dependence on the stress-strain response in these materials as shown in Fig. 1 and Fig. 2 and similar results published elsewhere [1-3]. In general it is well known and published that the mechanical properties of PBX 9501 also depends on many variables such as compaction density, processing methods, polymer characteristics (e.g. molecular weight), and relative humidity of storage environment to name a few relevant variables [4,5]. PBXs are formulated with a soft phase polymeric binder system mixed with hard phase explosive to facilitate processing, and to reduce the sensitivity to various stimuli. The material PBX9501 used in this study is comprised of approximately 95 wt% HMX, nearly 5 wt% binder and nitro plasticizer, and approximately 0.1 wt% stabilizers.

Despite these challenges, the micromechanical behavior of these particulate composite energetic materials has been extensively studied and

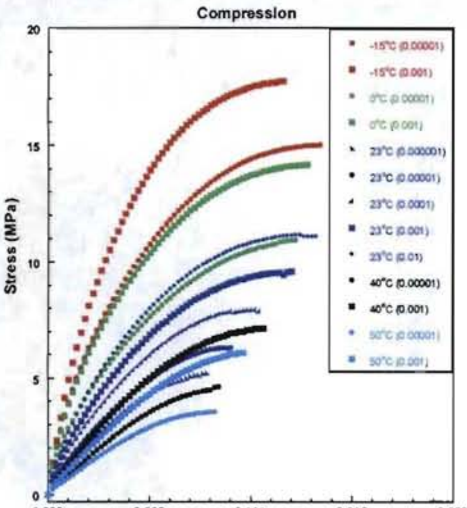

Fig. 1: Compressive Stress-Strain Curves for PBX 9501

constitutive models have been developed to at least partially describe the observed mechanical behaviors [2-3,6-11]. One particular micromechanical model of interest here is the ViscoSCRAM rate-dependent viscoelastic continuum damage model. This model is not a micromechanical in the sense that all constituents are explicitly modeled, but in the sense that a micro-mechanism namely microcracking, is used to account for nonlinear behavior and softening observed. The model has been used to simulate the thermal and mechanical behavior of plastic bonded explosives (PBXs) and study non-shock ignition (formation of explosive hot spots) [2-3]. The ViscoSCRAM material model has been used to simulate both dynamic and quasi-static behavior and has been validated against several experimental tests [2-3, 12]. However, despite these successes the model is severely limited to capturing the mechanical behavior up to or near failure and for the success of the validation may require further calibration of the parameters for each case of validation. That is, it is not truly predictive.

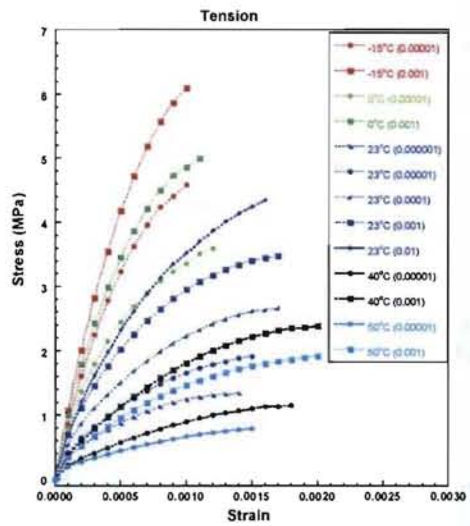

Fig. 2: Tensile Stress-Strain Curves for PBX 9501

The focus of this paper is to show the range of applications of the ViscoSCRAM material model in the quasi-static and dynamic regimes and to propose an alternative approach to fully capture the thermo-mechanical response of PBXs in regions where this model should not be applied. We start by briefly reviewing the ViscoSCRAM model theory and its range of applications as provided in references [2-3,12].

Theory

The ViscoSCRAM material model has been developed to model the following observed characteristics of PBX 9501; 1) irreversible material damage, 2) visco-elastic material response, 3) adiabatic mechanical heating, 4) chemical heating, and 5) nonshock ignition. This material model was developed by Bennett et al. [2] for explicit finite element applications and by Hackett and Bennett [3] for implicit finite element implementations. The underlying principles of both methods are identical. Off interest to this paper is the mechanical response portion of ViscoSCRAM. This is accomplished by coupling an isotropic material damage model with an isotropic, generalized Maxwell visco elastic model. The constitutive model separates the material response into volumetric and deviatoric components. By assuming that the simulations only see low pressure, a volumetric response characterized by a constant bulk modulus is sufficient. If large pressures were to obtain, as in shock loading cases, this assumption would be need to be removed. The deviatoric response is divided into two components acting in series with each other.

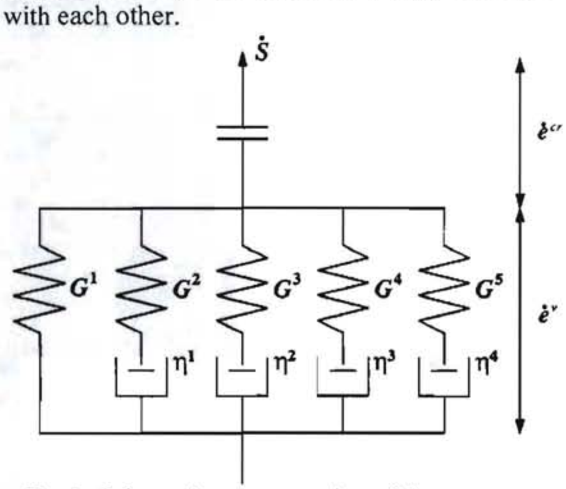

Fig. 3: Schematic representation of the ViscoSCRAM material model

One component is modeled as N Maxwell spring and dashpot elements acting in parallel to each other (where N is any integer). This component produces a viscoelastic response. A Maxwell spring and dashpot element is the ideal behavior of a linear spring and linear dashpot acting in series with each other. The spring is characterized by its contribution to the shear modulus of the material while the dashpot has characteristic relaxation time. For deformations occurring more rapidly than the characteristic time, the Maxwell element adds its stiffness to the other elements. For deformations on a time scale much longer than the characteristic time, the Maxwell element adds no stiffness.

In series with the viscoelastic component is a fracture mechanics based, continuum damage component. Addessio and Johnson [11] developed this model as a simplification of a statistical crack mechanics model of Dienes [13]. The model is characterized by a critical stress intensity factor, a mean crack size, an exponent that determines the crack growth velocity for conditions both below and above the critical stress intensity, and a maximum crack growth velocity. Model values are based on data from room temperature experiments on PBX-9501for quasi-static and high strain rates [1-3, 12, 15].

Shown in Fig. 3 is a one-dimensional conceptualization in which the visco elastic model is a spring connected in parallel with several spring/ dashpot elements, this is then connected in series with the damage model. In the figure, **S** refers to stress, **G** refers to stiffnesses, and η refers to viscous response parameters (viscosity). The total deviatoric strain rate is then the sum of the viscoelastic deviatoric strain rate, $\dot{\boldsymbol{\varepsilon}}^{v}$, plus the deviatoric damage strain rate, $\dot{\boldsymbol{\varepsilon}}^{cr}$. This generalization is assumed to apply in three dimensions. The theoretical development is somewhat involved so the reader is referred to further explanation provided in references [2-3].

As mentioned above, the focus of this paper will be on the mechanical response of PBX 9501. In this regard even though the ViscoSCRAM material model has been shown to simulate both quasi-static and high strain rates (from Hopkinson bar experiments) mechanical response, it should be mentioned that the model parameters are obtained from uniaxial compression measurements. An ad-hoc tensile damage growth rate factor is used to simulate the uniaxial tension response which as shown in Fig. 2 also shows rate dependence but with peak strength values lower than in compression. In addition there is no damage surface and damage accrues at a small finite rate only if shear and/or tensile stresses are present. The damage growth law is based on average microcrack radius, pressure, effective (deviatoric) strain rate, and von Mises stress. This seems to work fine as long as the loading is applied monotonically. This model will fail during cyclic loading even if it just a simple case of load and unload. This is because the damage parameter is continually updated as a function of load and there is a no deactivation for this parameter during the unload part of the cycle. This leads to a faster accrual of damage which leads to reaching the failure strength prematurely. For more details the reader is referred to equations 21 – 28 of reference [3]. The damage parameter is further explained in the results section under Example:3 Brazil Compression Disk.

In the next section on validation we provide three examples of the application of the ViscoSCRAM material model. The examples provide a comparison of the macroscopic response between the experiments and the model and as in the case of the Brazil disk test, strain contours at a small scale are also provided for comparison.

Results

Validation of ViscoSCRAM material model

Once the ViscoSCRAM material model is calibrated based on uniaxial compression and tension data from both quasi-static and dynamic strain rate tests, it is important to validate the model against know multiaxial measurements which provide a way of showing how good the material model is. Details of the calibration procedure are outlined in references [2-3].

The first example of three-point bending simulation is taken from the reference of [2-3]. The second example of a dynamic loading is taken from the unpublished work of the same authors [12]. The third example on Brazilian Disk geometry is a result of our work motivated by comparison with multidimensional strain measurements, macroscopic deformation and load changes as well as comparing damage with micro-structural images as offered by digital image correlation (DIC) techniques.

Example 1: Three-point Bending (Quasi-static loading) [3].

The first example application of the material model to PBX 9501 is a characterization of the behavior of the crack growth portion of the model. This is done by driving that portion of the material model with uniaxial loading applied to a three dimensional ABAQUS implicit finite element model consisting of a single element to obtain the relationship between crack growth rate and effective deviatoric strain with a threshold value of stress intensity and a maximum value of crack growth rate set to fixed values [3].

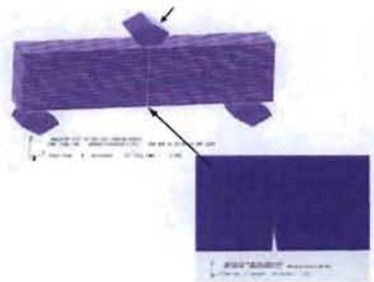

Fig. 4: Three-point bend specimen with a notch.

The three-point bend specimen is 75mm long, 15mm deep and 10mm wide, with a 2 mm saw cut in the center to initiate fracture. The finite element mesh of the 3 point bend test geometry with the zoomed in detail of the notch is shown in Fig. 4. As the load is applied with the plunder loading rate of 0.0212mm/s, Fig. 5 shows that a 'damage region' propagates from the notch vertically through the specimen at peak load, before any discrete fracture can be detected. As the center region is damaged, the load required to continue to move the plunger downward under displacement control decreases. Fig. 5 shows the σ_{11} stress field along the centre region of the mesh as the peak stress is reached. As the stress redistributes because of tensile damage along the vertical plane of maximum moment (x=l/2), the load carrying capability of the specimen decreases. The plunger load versus the centre beam deflection is shown in Fig. 6 from the finite element analysis, along with one set of test data for a test conducted at room temperature with a plunger loading rate of 0:0212mm/s. The comparison of the loading stiffness, the peak load and softening is good and shows that the crack growth micromechanics model is applicable for this type of study.

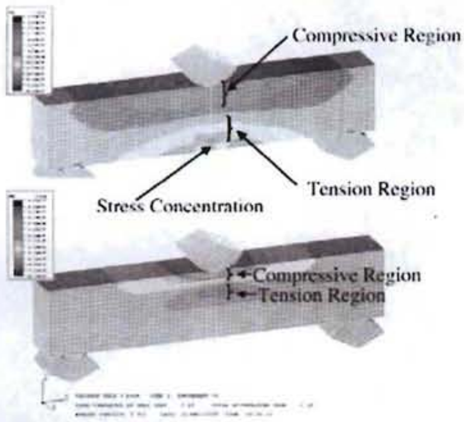

Fig. 5: Stress contours.

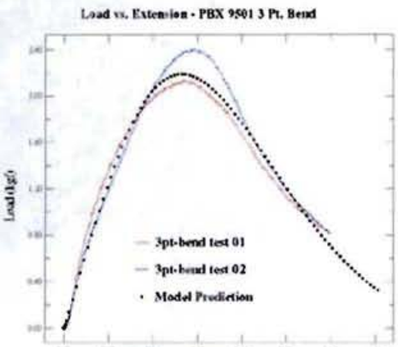

Fig. 6: Load extension plots (model vs. experiment).

Example 2: Split-Hopkinson Pressure Bar - Dynamic Loading:

In this example it is shows that modeling the Split-Hopkinson Pressure Bar (SHPB) test. This example is used as a validation of dynamic loading [12].

The finite element model mesh configuration of the Split-Hopkinson Pressure Bar (SPHB) test geometry is not shown here because the length scale compared to the bar diameters is so large that it appears only as a line, graphically. However, a "zoom-in" on the PBX 9501 specimen as modeled is shown in Fig. 7. The strain gages in this model are simulated at the midpoint of the incident-wave and transmitted-wave bars using thin shell or membrane elements that share the same nodes as the continuum elements that make up the outer surface at these locations. Their properties (modulus, thickness, etc) are set such that they contribute no stiffness to the elements to which they are "bonded". These elements simply follow the titanium bar motion, just as strain gages do.

Fig. 7: Finite Element Mesh of the "zoom-in" region.

The validation methodology used here is to compare the recorded strain gage time histories measured on the incident and transmitted pressure bars with the time history of the simulated strain gages in the finite element model. Fig. 8 illustrates these strain-time histories, with the upper record being that for the incident bar, and the lower record being that from the transmitted bar record. The titanium bars were modeled with no material damping, but it appears that from the higher frequencies, as evident in the strain gage records, the material does exhibit some damping. The agreement between the experimental record and the simulation is deemed remarkably well, and

Fig. 8: Comparison of the strain vs. time records

ViscoSCRAM is seen to capture the high rate response with good fidelity. It is not known at this time whether the difference between the records beginning at about 0.27 ms in the decay history for the transmitted wave can be improved upon with either more Maxwell elements or a slight change in the damage law or is due to experimental scatter. Although the peak dynamic strength has been demonstrated to be relatively constant for PBX 9501 [12], the micro-structural features vary from lot-to-lot which may also affect the global post-peak stress-time response. Thus, the simulation here is deemed excellent in agreement, and adequate to predict the structural response in continuum simulations.

The simulations illustrated in this example use ASC (Accelerated Scientific Computing) Technology and the LLNL (Lawrence Livermore National Laboratory) explicit FE program called PARADYN, a massively parallel version of DYNA3D [14]. The FE model contains about 2.1 million hexagonal 8-node brick continuum elements with about 65,000 elements in the PBX 9501 sample. The bar is modeled in quarter symmetry, with appropriate symmetry boundary conditions on the symmetry faces. All material interfaces are modeled as non-penetrating contact surfaces. The striker bar in this model is given an initial velocity corresponding to that of the test. It is remarked that, at Los Alamos National Laboratory, the striker bar velocity is not routinely measured. The breech chamber pressure for the gun that launches the striker bar is recorded, and a calibration curve is available to determine the striker bar velocity. However, the impact velocity can also be determined from the incident wave strain-time record. The average jump in strain for the incident wave form is related to the impact velocity, and this method was the used in this simulation to determine the initial velocity for the striker bar [12].

Example 3: Brazil Compression Disk

The deformation and failure of the pristine PBX 9501 high explosive is modeled and analyzed using the ViscoSCRAM material model.

The Brazilian disk compression provides a simple test configuration, where only internal cracks can be generated due to the compressive circumferential stress along the free surface. Brazilian disk compression involves a circular disk

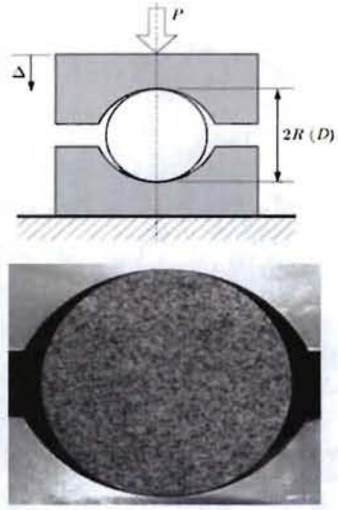

Fig. 9: Schematic of Brazil disk specimen and loading fixture

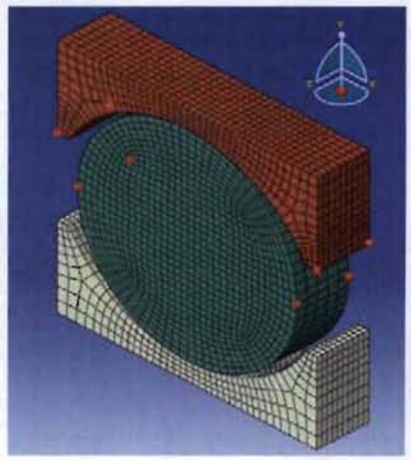

Fig. 10: FEM mesh Brazil disk specimen and loading fixture

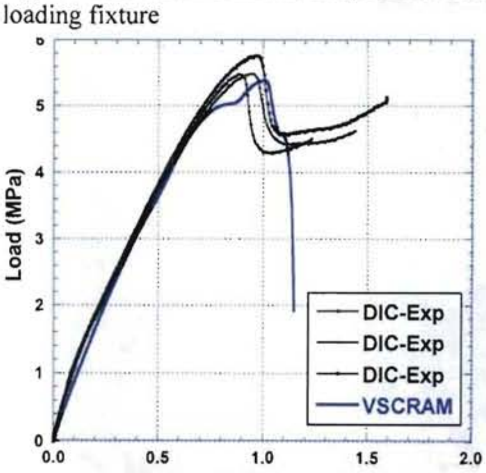

Fig. 11: Comparison between Load vs. Displacement plots.

with a pair of compressive forces acting across the vertical diameter. Such a test configuration was first used as an alternative for measuring elastic constants of materials with very low tensile strength and later it was used to determine the tensile strength of brittle materials, e.g., concretes and rocks. It has also been used in studying micro -cracking of the PBX 9501 high explosive; To directly observe the evolution of the deformation field, the optical technique of digital image correlation (DIC) was used. The technique of combining the Brazilian disk and the DIC has been applied to PBX 9501. From the DIC technique it was observed that around the moment in time that the applied load reaches maximum, localized deformation starts at the two regions near the loading points. The localized deformation then proceeds along an irregular path toward the center of the specimen and coalesces. The DIC technique also allows the calculation of strain fields from the full-field deformation field on the sample surface along with the overall deformation of the disk specimen. This type of technique lends itself very useful for validation of the ViscoSCRAM material model. We can now not only compare the overall comparison of the macroscopic behavior (e.g. Load vs. Displacement), but also surfaces strains (parallel and perpendicular to the loading direction) and as well correlate the damage parameter with that of the macroscopic cracking observed in the tests.

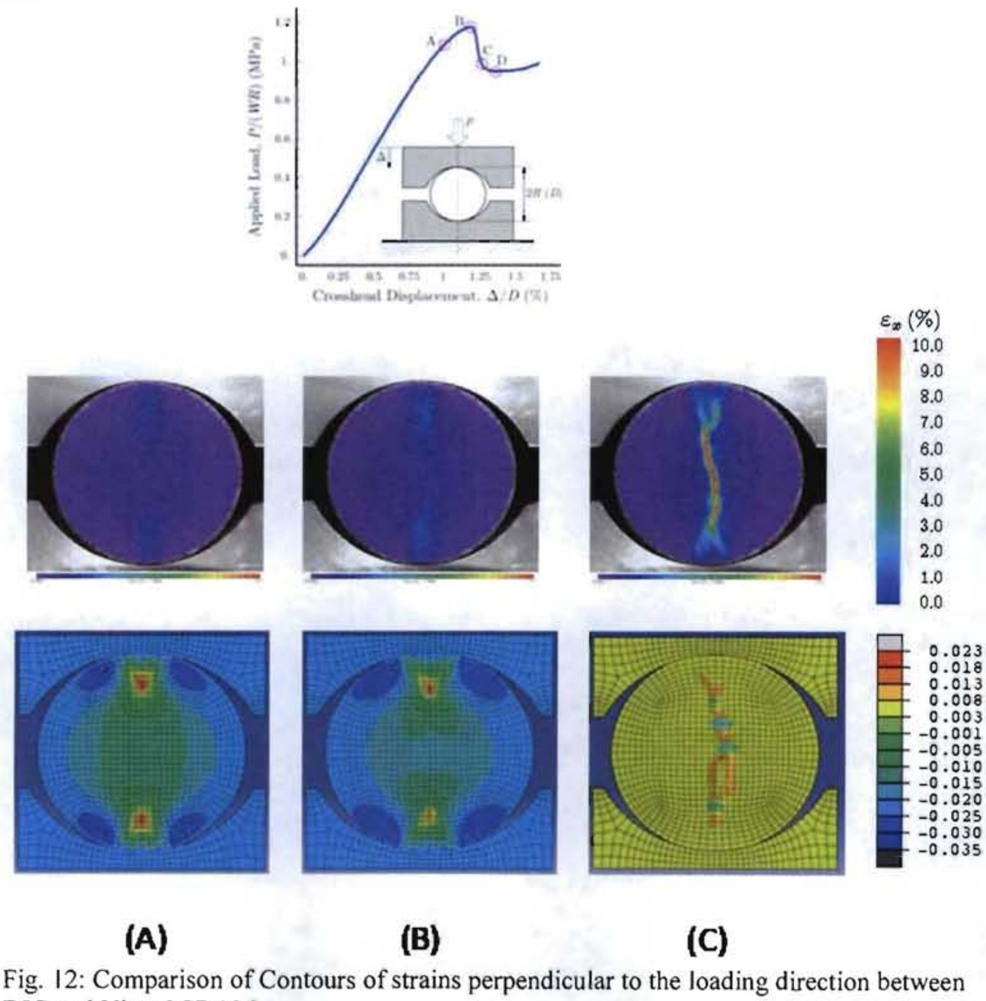

Fig. 12: Comparison of Contours of strains perpendicular to the loading direction between DIC and ViscoSCRAM

Finite Element Model

The Brazilian disk used in this study has the nominal dimension of 25.3 mm in diameter and 6.00 mm in thickness. A loading fixture with circular anvil is used for applying compressive load to the specimen (Fig. 9a). The radii ratio of the circular anvil and the circular disk is 1.25:1. On the surface of the disk specimen, a random speckle pattern was painted by spraying a black paint, as shown in Fig. 9b. The finite element mesh of the loading fixture and the disk specimen is shown in Fig. 10.

The assembly model was meshed using nearly 20,084 standard eight-node linear brick elements with a total of over 11,520 nodes. The numerical simulations focused on the mechanical response of the Brazilian Disk, especially the distribution of stress and strain across the center section of the disk. Fig. 11 show reaction force vs. displacement as measured and calculated from the finite element model. The experimental results show a peak load around 5.5 MPa and a peak displacement around 0.9 mm. The FE simulations show good agreement between the test results and ViscoSCRAM material model.

Fig. 12 shows the comparison of the experimental Digital image correlation (DIC) measurements of strain and ViscoSCRAM simulation along the direction perpendicular to the loading direction. The DIC technique relies on the computer vision approach to extract the whole field displacement data, that is, by comparing the features in a pair of digital images of a specimen surface before and after deformation. The measured and the calculated strains are shown to be tensile and is around 2% at the peak load shown as B in the figure above the DIC measurements of strain and ViscoSCRAM contour simulations along the direction perpendicular to the measurements. Even though beyond the peak load point the predictions from ViscoSCRAM are invalid it is still interesting to observe the capture of localization and propagation as observed from the experiment.

Fig. 13 shows the variation of the damage parameter with loading moment. Damage here is defined as the ratio of the initial crack radius to the size of the side of an arbitrary volume of some length sufficient large to keep the subsequent

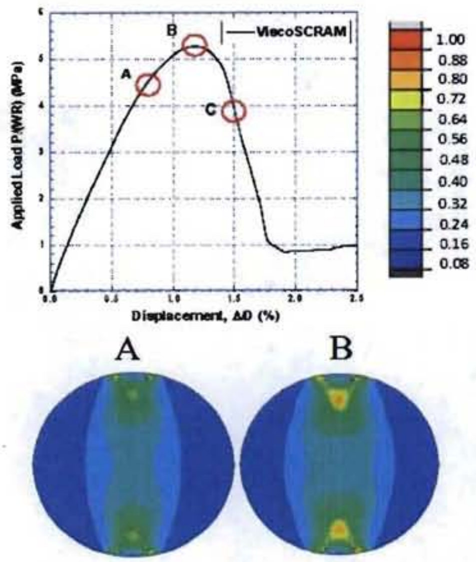

Fig. 13: Contours of ViscoSCRAM damage parameter

growth of the crack within the volume and is a scalar variable. Damage variable continuously increases in magnitude with loading and contributes to the degradation of the stiffness. The dimensionless damage parameter, $\bar{c}/a_o$ is in a range from 1.3 to 2.1. $\bar{c}$ is the average crack size and a_o is the length of a side of an arbitrary cube shaped volume containing the crack. This flavor of the damage parameter, while dimensionless, is not the classic damage parameter D by which stiffness parameter is degraded linearly as follows:

$$G^* = (1-D)G \qquad (1)$$

Such a damage parameter may be obtained by the following nonlinear conversion:

$$D = \frac{\left(\bar{c}/a_o\right)^3}{1+\left(\bar{c}/a_o\right)^3} \qquad (2)$$

When this conversion is performed, the damage parameter calculation at the peak stress (in uniaxial compression) is in the range of 0.67 to 0.9).

Discussion

What we have shown so far is to examine the validity of using the ViscoSCRAM material model for a range of mechanical tests. Our observations are that with careful calibration of the uniaxial test data, in general the reproducibility of tests subjected to monotonic loading up to failure is well captured. In addition for tests which have substantial hydrostatic loadings, the model does not apply because the damage evolution law is based on a deviatoric stress state. The effects of pressure are not included in the ViscoSCRAM model and it is clear from triaxial data that pressure has a big influence on the inelastic deformation as observed from triaxial tests (Fig. 14), where hydrostatic pressures can prevent the shear-enhanced dilatancy seen in axial compression tests This comes as no surprise as PBX 9501 is a granular material.

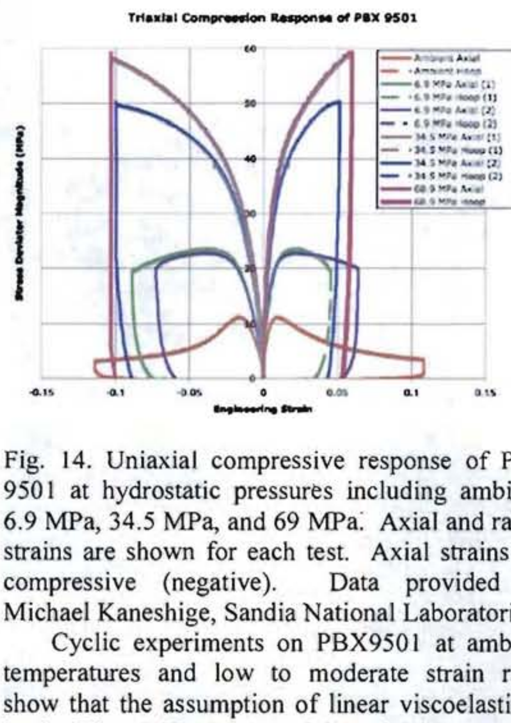

Fig. 14. Uniaxial compressive response of PBX 9501 at hydrostatic pressures including ambient, 6.9 MPa, 34.5 MPa, and 69 MPa. Axial and radial strains are shown for each test. Axial strains are compressive (negative). Data provided by Michael Kaneshige, Sandia National Laboratories.

Cyclic experiments on PBX9501 at ambient temperatures and low to moderate strain rates show that the assumption of linear viscoelasticity in the ViscoSCRAM material model is not valid. In addition to damage in the form of microcracks there is evidence of inelastic strain indicating the presence of other inelastic mechanisms such as plasticity and granular material mechanics which should be considered along with rate and temperature dependence. Evidence for this inelastic deformation is presented in Fig. 15, showing cyclic uniaxial compression test results on PBX 9501 with recovery times of approximately 50 minutes between cycles

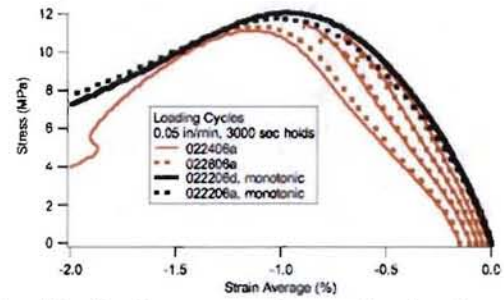

Fig. 15. Cyclic compression results showing the loading curves on two samples. Monotonic test results on two other samples are also shown. Between each pair of loading phases, samples were allowed to recover at low stress levels for 50 minutes. Data provided by Darla Graff Thompson, Los Alamos National Laboratory.

At this point, there is not sufficient evidence to specify the appropriate damage mechanism or damage evolution law for fully three-dimensional states at moderate to elevated temperatures and low to moderate strain rates. Previous consideration of highly filled materials with disparate properties between phases suggests that some damage is associated with inelastic volumetric growth, which would be suppressed at high pressures. If volumetric plastic strain is a damage mechanism, then it should affect volumetric compressibility. Triaxial data with separate unload and recovery data for uniaxial and hydrostatic loadings will allow us to identify this. The damage evolution laws postulated here will likely need to be modified and a pressure dependent flow law will likely need to be developed. Seminal work by Alek Zubelewicz suggests forms for the flow law and possibly the damage evolution law.

Concluding remarks

We have shown and discussed the validity of the ViscoSCRAM material model as supported by the examples on; 1) three-point bending, 2) Split Pressure Hopkinson Pressure Bar and 3) the Brazil Disk tests.

The ViscoSCRAM material model can be used to model monotonic non-linear behavior with softening for energetic materials stress states which are mainly uniaxial (or strongly deviatoric) in nature with minimal influence of pressure.

To fully model the three-dimensional states and the effects of elevated temperatures and low strain rates and add pressure dependence requires modification of the current damage evolution laws and also identify the appropriate damage mechanisms by carefully scoped experiments.

Acknowledgements

We would like to acknowledge NNSA's Advanced Simulation and Computing (ASC), Materials and Physics Program; and the Joint DoD/DOE Munitions Technology Development Program, for financial support. We also like to acknowledge the work of Zukun Chen who helped with the finite element analysis of the Brazilian Disk tests.

References

1. Idar D.J., Thompson, D.G., Gray III, G.T., Blumenthal, W. R., Cady, C.M., Peterson, P. D., Roemer, E.L., Wright, W.J., and Jacquez, B. L., "Influence of Polymer Molecular Weight, Temperature, and Strain Rate on the Mechanical Properties of PBX 9501", in M. Furnish, N. Thadhani, and Y. Horie, (Eds), AIP Conference Proceedings, American Institute of Physics, Melville, New York, p. 821, 8 July 2002.

2. Bennett, J.G., Haberman, K.S., Johnson, J.N., Asay, B.W., Henson, B.F., "A constitutive model for the non-shock ignition and mechanical response of high explosives". Journal of the Mechanics and Physics of Solids 46, 2303–2322. 1998.

3. Hackett, R.M., Bennett, J.G., 2000. An implicit finite element material model for energetic particulate composite materials. International Journal for Numerical Methods in Engineering 49, 1191–1209.

4. R. V. Browning, T. O. Meyer, Effects of Humidity and Other Variables on the Strength of PBX 9501, 23th Aging, Compatibility, and Stockpile Stewardship Conference Proceedings, Sandia National Laboratories, SAND2001-8038, CA, November 14 – 16 2000, p. 69.

5. R. V. Browning, T. O. Meyer, Effects of Reduced Nitroplasticizer Content on the Compressive Strength of PBX 9501, Report PXRPT-05-03, 2005, BWXT Pantex Plant, Amarillo, TX, USA.

6. S.G. Bardenhagen, J.U. Brackbill, Journal of Applied Physics 83, 5732–5740, 1998.

7. S.G. Bardenhagen, J.U. Brackbill, D. Sulsky, Computational Methods in Applied Mechanics and Engineering 187, 529–541, 2000.

8. B.E. Clements, E.M. Mas, Journal of Applied Physics 90, 5522–5534, 2001.

9. B.E. Clements, E.M. Mas, Modelling and Simulation in Materials Science and Engineering 12, 407–421, 2004.

10. B. Banerjee, C.M. Cady, D.O. Adams, Modelling and Simulations in Materials Science Engineering 11, 457–475, 2003.

11. Addessio, F.L., Johnson, J.N., A constitutive model for the dynamic response of brittle materials. Journal of Applied Physics 67, 3275–3286. 1990.

12. Bennett, J.G., Gray III, G.T., Blumenthal R. W., "Validation of Complex Rate-Dependent Material Constitutive Models", LA-UR-01-1711, 2001.

13. Dienes, J.K., "Strain-softening via SCRAM", Los Alamos National Laboratory Report., LA-UR-98-3620, 1998.

14. DYNA3D, UCRL-MA-107254, LLNL, 1993

15. Gray III, G.T., Blumenthal, W.R,. Cady, C.M. and Idar, D.J, "Influence of Temperature on the High-Strain-Rate Mechanical Behavior of PBX 9501 and PBXN-9," presented at the 1997 Topical Group on Shock Compression Meeting, Amherst, MA, 27 July-1 August 1997.

16. ABAQUS, Standard User's and Theory Manuals. Version 6.7, DS Simulia, Providence, RI, 2007.